OGLE2-TR-L9b: An exoplanet transiting a fast-rotating F3 star*

Snellen I.A.G.[1], Koppenhoefer J.[2,3], van der Burg R.F.J.[1], Dreizler S.[4], Greiner J.[3], de Hoon M.D.J.[1], Husser T.O.[5], Krühler T.[3,6], Saglia R.P.[3], Vuijsje F.N.[1]

[1] Leiden Observatory, Leiden University, Postbus 9513, 2300 RA, Leiden, The Netherlands
[2] Universitäts-Sternwarte München, Munich, Germany
[3] Max-Planck-Institut für extraterrestrische Physik, Giessenbachstrasse, D-85748 Garching, Germany
[4] Institut für Astrophysik, Georg-August-Universität Göttingen, Friedrich-Hund-Platz 1, 37077 Göttingen, Germany
[5] South African Astronomical Observatory, P.O. Box 9, Observatory 7935, South Africa
[6] Universe Cluster, Technische Universität München, Boltzmannstraße 2, D-85748, Garching, Germany

ABSTRACT

Context. Photometric observations for the OGLE-II microlens monitoring campaign have been taken in the period 1997−2000. All light curves of this campaign have recently been made public. Our analysis of these data has revealed 13 low-amplitude transiting objects among ∼15700 stars in three Carina fields towards the galactic disk. One of these objects, OGLE2-TR-L9 (P∼2.5 days), turned out to be an excellent transiting planet candidate.

Aims. In this paper we report on our investigation of the true nature of OGLE2-TR-L9, by re-observing the photometric transit with the aim to determine the transit parameters at high precision, and by spectroscopic observations, to estimate the properties of the host star, and to determine the mass of the transiting object through radial velocity measurements.

Methods. High precision photometric observations have been obtained in g', r', i', and z' band simultaneously, using the new GROND detector, mounted on the MPI/ESO 2.2m telescope at La Silla. Eight epochs of high-dispersion spectroscopic observations were obtained using the fiber-fed FLAMES/UVES Echelle spectrograph, mounted on ESO's Very Large Telescope at Paranal.

Results. The photometric transit, now more than 7 years after the last OGLE-II observations, was re-discovered only ∼8 minutes from its predicted time. The primary object is a fast rotating F3 star, with $v\sin i$=39.33±0.38 km/s, T=6933±58 K, log g = 4.25±0.01, and [Fe/H] = −0.05±0.20. The transiting object is an extrasolar planet with M_p=4.5±1.5 M_{Jup} and R_p=1.61±0.04R_{Jup}. Since this is the first planet found to orbit a fast rotating star, the uncertainties in the radial velocity measurements and in the planetary mass are larger than for most other planets discovered to date. The rejection of possible blend scenarios was based on a quantitative analysis of the multi-color photometric data. A stellar blend scenario of an early F star with a faint eclipsing binary system is excluded, due to the combination of 1) the consistency between the spectroscopic parameters of the star and the mean density of the transited object as determined from the photometry, and 2) the excellent agreement between the transit signal as observed at four different wavelengths.

Key words. stars: planetary systems - techniques: photometric - techniques: radial velocity

1. Introduction

Transiting extrasolar planets allow direct measurements of their fundamental parameters, such as planet mass, radius, and mean density. Furthermore, their atmospheres can be probed through secondary eclipse observations (e.g. Charbonneau et al. 2005; Deming et al. 2005; Knutson et al. 2007), and atmospheric transmission spectroscopy (e.g. Charbonneau et al. 2002; Tinetti et al. 2007; Snellen et al. 2008). This makes transiting exoplanets of great scientific value.

Many photometric monitoring surveys are currently underway. Several of these surveys are very successful, such as the transit campaigns of the Optical Gravitational Lens Experiment (OGLE-III; 7 planets; e.g. Udalski et al. 2008), the Trans-Atlantic Exoplanet Survey (TrES; 4 planets; e.g. Mandushev et al. 2007), the Hungarian Automated Telescope Network (HATNet; 9 planets; e.g. Shporer et al. 2008), the XO survey (5 planets; e.g. Burke et al. 2007), and the Wide Area Search for Planets (SuperWASP; 15 planets; e.g. Anderson et al. 2008). In addition, CoRoT is targeting planet transits from space (4 planets; e.g. Aigrain et al. 2008), ultimately aimed at finding Earth or super-Earth size planets.

In this paper we present a new transiting extrasolar planet, OGLE2-TR-L9 b. The system has an I-band magnitude of I=13.97, and an orbital period of ∼2.5 days. The host star is the fastest rotating and hottest (main sequence) star around which an orbiting extrasolar planet has been detected to date. The transit system was the prime planetary candidate from a sample of thirteen objects presented by Snellen et al. (2007; S07). They were drawn from the online database of the second phase of the OGLE project, a campaign primarily aimed at finding microlensing events, conducted between 1997 and 2000 (OGLE-II; Szymanski 2005; Udalski et al. 1997). The low amplitude transits were discovered among the light curves of ∼15700 stars, with 13.0<I<16.0, located in three Carina fields towards the galactic plane. Note that the light curve data have a different cadence than usual for transit surveys, with 1−2 photometric points taken per night, totalling 500−600 epochs over 4 years. This work shows that such a data set is indeed sensitive to low-amplitude transits, and can yield transiting extrasolar planets.

In section 2 of this paper we present the analysis of new transit photometry of OGLE2-TR-L9, taken with the GROND instrument mounted on the MPI/ESO 2.2m telescope at La Silla. The particular goals of these observations are the re-discovery of the transit, improved transit parameters and orbital

OGLE2−TR−L9
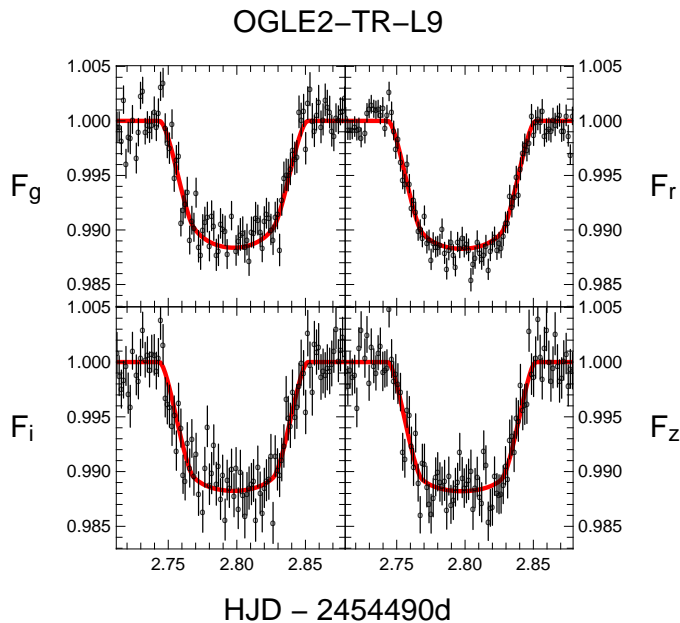
Fig. 1. Transit lightcurves of OGLE-TR-L9 in g′, r′, i′ and z′ observed simultaneously with the GROND instrument, mounted on the MPI/ESO 2.2m telescope. The line shows the best model fit for the combined light curves, as discussed in the text.

Table 1. Limb-darkening coefficients used for the transit fitting, taken from Claret (2004) for a star with metallicity $[Fe/H]$=0.0, surface gravity log g=4.5, and effective temperature T_{eff}=7000K.

filter	γ_1	γ_2
g′	0.3395	0.3772
r′	0.2071	0.3956
i′	0.1421	0.3792
z′	0.0934	0.3682

ephemeris. In section 3 the spectroscopic observations with the FLAMES/UVES multi-fiber spectrograph on ESO's Very Large Telescope are described, including a description of the analysis of the radial velocity variations, of the bisector span, and the spectroscopic parameters of the host star. In section 4 and 5 the stellar and planetary parameters with their uncertainties are determined, and arguments against a stellar blend scenario laid out. The results are discussed in section 6.

2. Transit photometry with GROND

2.1. Data acquisition and analysis

We observed one full transit of OGLE-TR-L9 with GROND (Greiner et al. 2008), which is a gamma ray burst follow-up instrument mounted on the MPI/ESO 2.2m telescope at the La Silla observatory. GROND is a 7-channel imager that allows to take 4 optical (g′r′i′z′) and 3 near infrared (JHK) exposures simultaneously. On January 27, 2008, a total of 104 images in each optical band and 1248 images in each near infrared band were taken. The JHK-images turned out to have insufficient signal to noise to detect the transit, and will not be considered further. Using exposure times of 66 seconds and a cycle rate of 2.5 minutes, we covered a period of about 4 hours centered on the predicted transit time. All optical images have been reduced with the *mupipe* software developed at the University Observatory

in Munich[1]. After the initial bias and flatfield corrections, cosmic rays and bad pixels were masked and the images resampled to a common grid. The frames did not suffer from detectable fringing, even in z-band. Aperture photometry was performed on OGLE2-TR-L9 and eight to ten interactively selected reference stars, after which light curves were created for each of the 4 bands. The aperture radius was chosen to be 12 pixels, corresponding to 1.9 arcseconds, with a seeing of typically 1.1 arcseconds during the observations. The sky was determined in an annulus between 20 and 30 pixels from the object positions. The rms in the individual light curves of the reference stars was in all cases better than 0.3%. This resulted in typical precisions of the relative fluxes better than 0.2%.

2.2. Fitting the transit light curves

The lightcurves in g′, r′, i′, and z′, were fitted with analytic models as given by Mandel & Agol (2002). We use quadratic limb-darkening coefficients taken from Claret (2004), for a star with metallicity [Fe/H]=0.0, surface gravity log g=4.5, and effective temperature $T_{\rm eff}$=7000K (very close to the spectroscopic parameters of the star as determined below). The values of the limb-darkening coefficients are given in Table 1. Using a simultaneous fit to all 4 lightcurves we derived the mean stellar density, $M_{\rm star}$ / $R_{\rm star}^3$ in solar units, the radius ratio $R_{\rm planet}$ / $R_{\rm star}$, the impact parameter $\beta_{\rm impact}$ in units of $R_{\rm star}$, and the timing of the central transit. Together with a scaling factor for each band, there were eight free parameters to fit.

The light curves and the model fits are shown in Fig. 1., and the resulting parameters are listed in Table 2. All lightcurves fit well to the model except for the g-band lightcurve, which is attributed to the significantly more noisy light curve, and the poorly determined baseline, particularly before ingress.

3. Spectroscopic Observations with UVES/FLAMES

We observed OGLE2-TR-L9 with the UV-Visual Echelle Spectrograph (UVES; Dekker et al. 2000), mounted at the Nasmyth B focus of UT2 of ESO's Very Large Telescope (VLT) at Paranal, Chile. The aims of these observations were to estimate the spectroscopic parameters of the host star, and to determine the radial velocity variations. The observations were performed in fiber mode, with UVES connected to the FLAMES fiber facility (Pasquini et al. 2002), with 7 science fibers and with simultaneous thorium-argon wavelength calibration (*UVES7 mode*). Apart from our main target, fibers were allocated to two other OGLE-II transit candidates from S07 (OGLE2-TR-L7 and OGLE2-TR-L12), and three random stars within the 25′ FLAMES field. In addition, one fiber was positioned on empty sky. A setup with a central wavelength of 580 nm was used, resulting in a wavelength coverage of 4785−6817Å over two CCDs, at a resolving power of R=47000. Since the upper CCD turned out to cover only a small number of strong stellar absorption lines, in addition to suffering from significant telluric contamination, only the lower CCD (4785−5729Å) was used for further analysis.

Eight observations were taken in Director's Discretionary Time, in service mode in the course of December 2007 and January 2008, spread in such a way that the data would be evenly distributed in orbital phase of our main target (see table 3). The data were analysed using the *midas*-based UVES/FLAMES

---

[1] http://www.usm.lmu.de/~arri/mupipe/
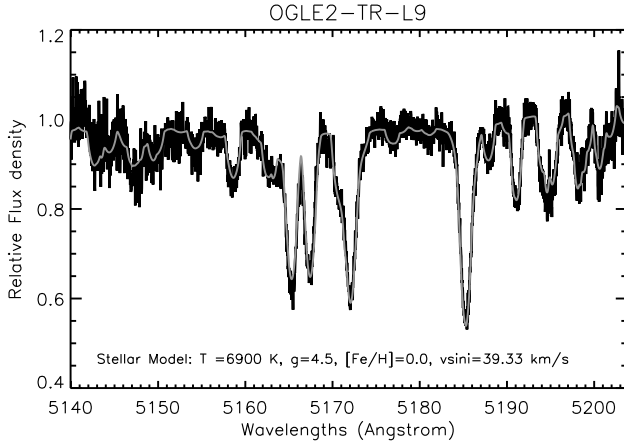
Fig. 2. The central part of one order of the combined UVES spectrum of OGLE2-TR-L9, with overplotted a synthetic spectrum with T=6900 K, g=4.5, [Fe/H]=0, and vsini = 39.33 km/sec.

Table 2. The transit, host star, and planetary companion parameters as determined from our photometric and spectroscopic observations.

Transit:		
ρ_s	=	0.4260±0.0091 ρ_{sun}
R$_p$/R$_s$	=	0.10847±0.00098
β_{impact}	=	0.7699±0.0085
t$_0$	=	2 454 492.79765±0.00039 HJD
P	=	2.4855335±7×10^{-7} d
Host star:		
Coord. (J2000)	=	11$^{\mathrm{h}}$ 07$^{\mathrm{m}}$ 55.29$^{\mathrm{s}}$ −61° 08′ 46.3″
I mag	=	13.974
I−J mag	=	0.466±0.032
J−K mag	=	0.391±0.049
T	=	6933±58 K
log g	=	4.47±0.13*
log g	=	4.25±0.01**
[Fe/H]	=	−0.05±0.20
vsini	=	39.33±0.38 km/s
R$_s$	=	1.53±0.04 R$_{\mathrm{sun}}$
M$_s$	=	1.52±0.08 M$_{\mathrm{sun}}$
Age	<	0.66 Gyr
Planetary Companion:		
K	=	510±170 m/s
i	=	79.8±0.3°
a	=	0.0308±0.0005 AU
R$_p$	=	1.61±0.04 R$_{\mathrm{jup}}$
M$_p$	=	4.5±1.5 M$_{\mathrm{jup}}$

*Determined from the spectroscopic analysis
**Determined from mean stellar density combined with the
  evolutionary tracks

pipeline as provided by ESO, which results in fully reduced, wavelength calibrated spectra. Since we were concerned about the wavelength calibration of the fifth epoch (see below), we also analysed the data using purpose-build IDL routines. No significant differences in the wavelength solutions were found. The resulting signal-to-noise per resolution element, in the central part of the orders, varies between ~10 and 20 over the different epochs (see table 3).

Table 3. Spectroscopic observations of OGLE2-TR-L9 taken with UVES/FLAMES. The first three columns give the Heliocentric Julian Date, the planet's orbital phase at the time of observation, and the signal-to-noise ratio of the spectra per resolution element in the center of the middle order. Column 4 and 5 give the radial velocity and the bisector span measurements.

HJD −2450000	Orbital Phase	SNR	RV km s^{-1}	BiS km s^{-1}
4465.8421	0.157	19.0	1.090±0.224	-0.076±0.482
4466.8583	0.566	16.6	1.204±0.276	0.173±0.380
4468.7219	0.316	11.2	0.842±0.212	-0.233±0.683
4472.7447	0.934	14.7	1.105±0.231	-0.492±0.460
4489.6749	0.746	9.0	2.345±0.376	0.123±1.101
4490.8382	0.214	15.3	0.472±0.318	0.235±0.339
4493.7697	0.393	19.9	1.187±0.187	-0.150±0.432
4496.7703	0.601	19.0	1.190±0.272	0.418±0.545

3.1. Determination of stellar spectroscopic parameters

The spectroscopic parameters of the star, vsini, surface temperature, surface gravity, and metallicity, were determined from the SNR-weighted, radial velocity shifted combination of the eight epochs taken with UVES. This combined spectrum has a signal-to-noise ratio of ~42 in the central areas of the orders. Detailed synthetic spectra were computed using the interactive data language (IDL) interface SYNPLOT (I. Hubeny, private communication) to the spectrum synthesis program SYNSPEC (Hubeny et al. 1995), utilising Kurucz model atmospheres[2]. These were least-squares fitted to each individual order of the combined UVES spectrum. The final atmospheric parameters were taken as the average values across the available orders. The uncertainties in the fitted parameters estimated using a χ-square analysis and from the scatter between the orders, give similar results, of which the latter are adopted.

The best fitting parameters and their uncertainties are given in table 2. One order of the combined UVES spectrum is shown in figure 2, showing the Mg$_b$ 5170Å complex, with the synthetic spectrum with T=6900 K, log g=4.5, [Fe/H]=0, and vsini = 39.33 km/sec, overplotted.

3.2. Radial velocity measurements

The orders of the eight spectra were first cosine-tapered to reduce edge effects. Cross-correlations were performed using the best-fitted velocity-broadened synthetic spectrum, as determined above, as a reference. The spectrum of the sky-fiber indicated that the sky contribution was typically of the order of ~0.5%. However, for the observation at 0.74 orbital phase (epoch 5), the relative sky levels were an order of magnitude larger, due to a combination of bad seeing and full moon. We therefore subtracted the sky spectrum from all target spectra before cross-correlation.

The resulting radial velocity data are listed in table 3, corrected to heliocentric values. The uncertainties are estimated from the variation of the radial velocity fits between the different orders. The final radial velocity data as function of orbital phase (the latter determined from the transit photometry), are shown in figure 3. The data were fitted with a sine function with the amplitude of the radial velocity variations, K, and a zero-point, V$_0$, as free parameters. The radial velocity amplitude was determined at K= 510 ± 170 m/s, with V$_0$=+0.2 km/s.

---

[2] http://kurucz.harvard.edu/grids.html
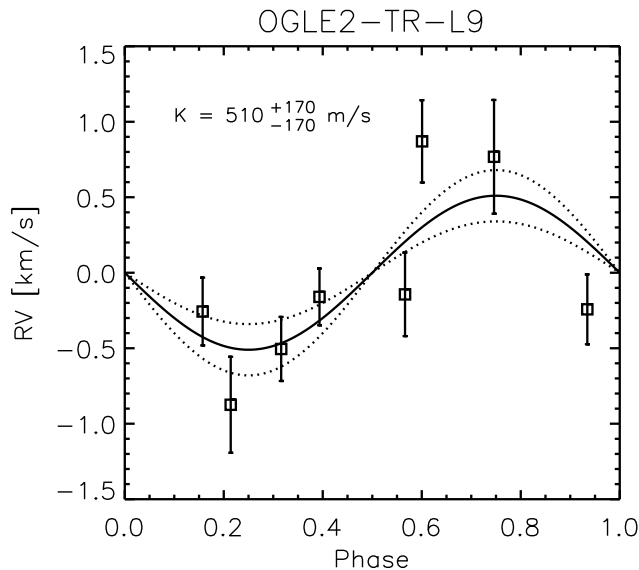
Fig. 3. The radial velocity measurements of OGLE2-TR-L9 as function of orbital phase from the ephemeris of the transit photometry.

We also determined the variations of the bisector span (following Queloz et al. 2001) as function of radial velocity and orbital phase. These are shown in figure 4. We least-squares fitted the bisector span measurements as function of orbital phase with a sinusoid, but no significant variations at a level of -0.01 ± 0.140 km s^{-1} are found. Although this means that there is no indication that the measured radial velocity variations are due to line shape variations, caused by either stellar activity or blends of more than one star, the errors are very large, making any claim based on the bisector span rather uncertain.

4. Estimation of the stellar and planetary parameters

4.1. Stellar mass, radius, and age

The transit photometry provides an estimate of the mean density of the host star, while the spectroscopic observations yield its surface temperature, surface gravity, and metallicity. The stellar evolutionary tracks of Siess et al. (2000) were subsequently used to estimate the star's mass, radius, and age, resulting in $M_s=1.52\pm0.08$ M$_{sun}$, $R_s=1.53\pm0.04$ R$_{sun}$, and an age of <0.66 Gyr. These parameters correspond to a surface gravity of log g = 4.25±0.01, which is in reasonable agreement, but about 1.7σ lower than the spectroscopic value. It should be realised that it is notoriously difficult to obtain reliable log g values from relatively low signal to noise spectra.

4.2. Planetary Mass and Radius

Using the values obtained from the transit fit to the GROND light curves, the radial velocity fit, and the stellar parameters as derived above, we obtain a planetary mass of $M_p = 4.5\pm1.5$ M$_{jup}$ and a planetary radius of $R_p = 1.61\pm0.04$ R$_{jup}$. The semi-major axis of the orbit is at a=0.0308±0.0005 AU. The mean density of the planet is 1.44±0.49 g cm^{-3}.

This means that OGLE2-TR-L9b is one of the largest known transiting hot Jupiters, only TrES-4b and WASP-12b are
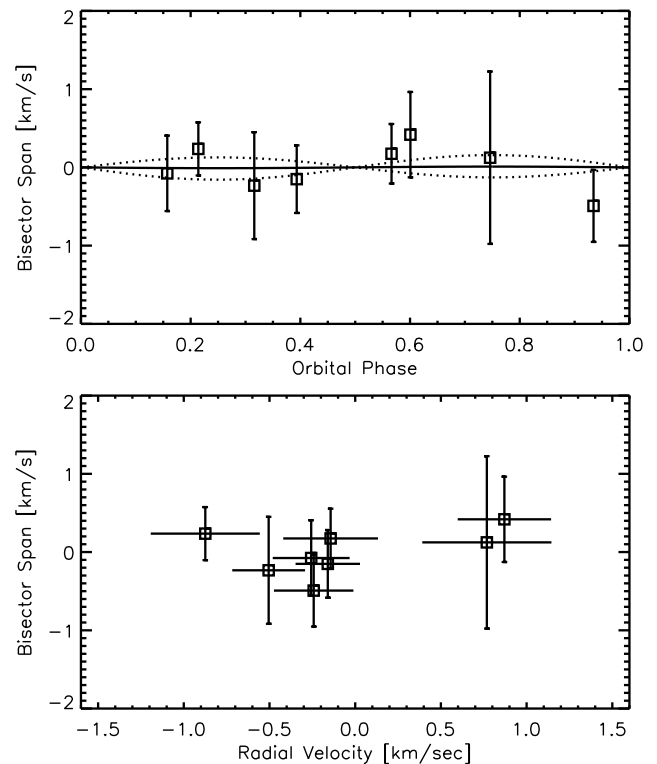
Fig. 4. Bisector variations as function of orbital phase (top panel) and radial velocity value (bottom panel). The solid line and dashed lines in the top panel indicate the least-squares fitted sinusoidal variation in the bisector span and its uncertainty at -0.01 ± 0.140 km s^{-1}.

marginally larger, although its mean density is similar to that of Jupiter. Even so, OGLE2-TR-L9b is significantly larger than expected for an irradiated ∼4.5 M$_{Jup}$ planet (Fressin et al. 2007).

5. Rejection of blended eclipsing binary scenarios

Large photometric transit surveys are prone to produce a significant fraction of false interlopers among genuine transiting extrasolar planets. If the light from a short-period eclipsing stellar binary is blended with that from a third, brighter star, the combined photometric signal can mimic a transiting exoplanet. Although the radial velocity variations induced by an eclipsing binary should be orders of magnitude larger than those caused by a planet, the blending of the spectral lines with those from the brighter, third star could produce variations in the overal cross-correlation profile that have significantly smaller amplitudes, possibly as small as expected for giant planets. Since this would be accompanied with significant line-shape variations, bisector span analyses are often used to reject a blended eclipsing binary scenario.

Although no significant variations in the bisector span are observed in OGLE2-TR-L9, it could be argued that this is due to the lack of signal-to-noise. We show however that a blended eclipsing binary scenario can be rejected anyway, because of the following observations:

1 Transit light curves from g′ to z′ band: As can be seen in Fig. 1, there is an excellent agreement between the light curves from g to z band. This means that if the transit was actually caused by a background eclipsing binary blended
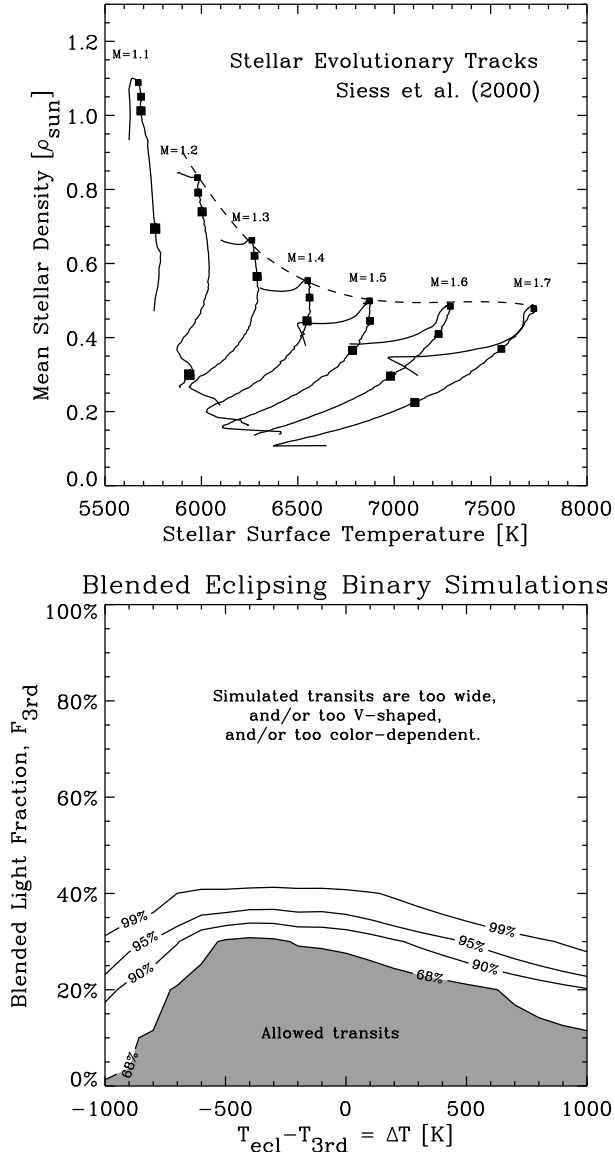
Fig. 5. The upper panel shows the stellar surface temperature, T_s, versus the mean density, ρ_s, for evolutionary tracks of Siess et al. (2000). The filled squares on each track indicate stellar ages of 0.1, 0.5, and 1×10^9 years, (and 5×10^9 years for $M{\le}1.2M_{Sun}$), with larger symbols indicated higher ages. The dashed line indicates the maximum possible ρ_s for a given stellar surface temperature. The bottom panel shows the confidence intervals from the χ-square analysis of all possible blended eclipsing binary scenarios fitted to the GROND light curves, with on the x-axis the difference in surface temperature between the eclipsed and the third star, and on the y-axis the fraction of the total light coming from the third star in r'-band. It shows that the combined g'r'i'z' light curves can only be fitted including a low level ($\lesssim$ 30%) of light contamination.

with a bright foreground star, the colors (and thus the surface temperatures) of the eclipsed binary star and foreground star should be very similar.

2 Transit shape and spectral classification: The mean stellar density as determined from the transit photometry is in excellent agreement with the spectral classification, both con-

sistent with an early F star. Using the argument above, this means that if this is a blend, then both the foreground star and the eclipsed binary star should be early F stars.

However, if we now assume that a significant fraction of the light comes from a foreground star, and we remove this contribution from the light curve, the transit can no longer be fitted by an early F star, but only by a star of significantly higher mean density, implying a cooler, less massive star, which is again in contradiction with point 1). This means that the early F star *is* the transited object, and that a blended eclipsing binary scenario can be rejected.

To further explore the possible role of additional light from a blended star, we performed a quantitative analysis, simulating background eclipsing binary systems with their light diluted by that from a third star. We first used the stellar evolutionary tracks of Siess et al. (2000) to determine the full range of stellar parameters that can be present in eclipsing binaries, of which only the stellar surface temperature, T_{ecl}, and the mean stellar density, ρ_{ecl} of the eclipsed star are of interest for the simulations. Note that the evolutionary status of the third star is not important, since we do not restrict ourselves to physical triple systems, but also include chance-alignments of back- and foreground stars. As is indicated in the top panel of figure 5, where the stellar evolutionary tracks are shown, there is a maximum possible mean-stellar density for a given surface temperature. This was used as a boundary condition in the simulations.

In our simulations we varied two parameters, 1) the difference between the surface temperature of the eclipsed star and that of the third star, ΔT (-1000 K$<\Delta T<+1000$ K), and 2) the fraction of light coming from the third (possibly unrelated) star, F_{3rd} ($0<F_{3rd}< 99\%$). The combined light of the eclipsing binary and third star should produce a spectrum which is best fitted with a surface temperature of $T_{comb} = 6933$ K. Therefore a simple linear relation between T_{comb} and the surface temperatures of the individual stars was assumed, such that $T_{ecl} = T_{comb} - \frac{F_{3rd}}{1+F_{3rd}}\Delta T$. Note that any small fraction of light that could be coming from the eclipsing star is simply added to F_{3rd}. In this way, each combination of F_{3rd} and ΔT, results in a T_{ecl} and a maximum possible ρ_{ecl}. It also results in a fractional contribution of light from the third star that varies over the four filters.

Subsequently, for each combination of F_{3rd} and ΔT, model eclipsing binary light curves were least-squares fitted to the g'r'i'z' GROND data, using as before the algorithms of Mandel & Agol (2002), in which the binary size ratio and the impact parameter were completely free to vary, and ρ_{ecl} was retricted to be below the upper limit set by T_{ecl}. In this way, all possible blended eclipsing binary scenarios are simulated, independently of whether the third star is physically related to the binary or not. The bottom panel of figure 5 shows the confidence contours of the χ-square analysis of all possible blended eclipsing binary scenarios. It shows that the combined g'r'i'z' data can only be fitted by light curves of eclipsing binaries with a low level $\lesssim$30% (90% confidence level) of blended light, meaning that most light in the stellar spectrum must come from the eclipsed star. Scenarios in which the stellar spectrum is dominated by a third star with a small contribution from a background eclipsing binary, can be strongly rejected. The transit light curves produced by those rejected scenarios are simply too wide, and/or too V-shaped, and/or too color dependent to fit the GROND data. One scenario that we cannot reject, is a small contribution from a blended star. For example, it could in principle be possible that the light from the transited F3 star is diluted at a ~30% level with light from another F star (with a similar v*sin*i and radial

velocity, otherwise it would show up in the spectra). In this case, the transiting planet would be ~30% more massive (and ~15% larger) than determined above, by no means moving it outside the planet mass range.

Note that for most transiting planets presented in the literature, such a low-level contamination scenario can not be excluded, since the variations in the bisector span would be orders of magnitude smaller than in the case of a blended eclipsing stellar binary. This is because the radial velocity variations in the latter case are 10^{2-3} times larger than in the first case.

There have been several reports of blended eclipsing binaries hiding out as transiting planets, most notably by Mandushev et al. (2005), and Torres et al. (2004). However, these studies dealt with very low signal-to-noise light curves, and the true nature of these systems would have been easily brought to light by such high quality photometric data as presented in this paper. Mandushev et al. (2005) rejected a transiting planet scenario for the fast rotating (vsini=34 km/s) F5 star GSC 01944-02289, in favour of a blended eclipsing binary. This system was shown to consist of a hierarchical triple composed of an eclipsing binary with G0V and M3V components, in orbit around a slightly evolved F5 dwarf. The latter star in this scenario contributes for ~89% to the total light from the system. Although they claim that the true nature of this system was not revealed by their BVI light curves, the color difference between the G0V and F5V star means that the transit must be 25-30% deeper in I-band than in B-band. However, no quantitative analysis of the light curves was presented, and the authors claim that the true nature of the system was only brought to light by spectroscopic means. In a similar fashion Torres et al. (2004) presented the case of OGLE-TR-33, which was identified as a triple system consisting of an eclipsing binary with F4 and K7-M0 components orbiting a slightly evolved F6 star. However, their photometry relied solely on the original I-band OGLE-III data, resulting in a relatively low SNR transit detection with the ingress and bottom of the transit not well covered. They also claim that the blended eclipsing binary is only revealed by spectroscopy. However, their best fitting planet model already pointed towards a very unlikely planet radius of ~3 R_{Jup}, and the V-shaped transit produced by the blended eclipsing binary would have been easily picked up by our high precision photometry. Note that while Torres et al. (2004) and Mandushev et al. (2005) only consider physical triple systems, our analysis presented above includes all possible scenarios, also those involving chance-alignment of background or foreground stars.

6. Discussion

More than seven years and >1000 orbital periods after the last observations of OGLE2-TR-L9, the transit signal was rediscovered only 8 minutes from its predicted time (from S07). It not only shows that an observing campaign with large time intervals between measurements can produce reliable light curves, it also shows it produces extremely accurate orbital periods.

OGLE2-TR-L9b is the first extrasolar planet discovered transiting a fast rotating (vsini=39 km/s) F star. OGLE2-TR-L9 is also the star with the highest surface temperature (T=6933 K) of all main sequence stars that host an exoplanet known to date. It is therefore not surprising that the uncertainties in the radial velocity variations are higher than for most other transiting exoplanets presented in the literature. Only due to the high mass of OGLE2-TR-L9b, we were able to detect its radial velocity signature. Note however that, since a blend scenario can be rejected at high significance, an upper limit to the mass of OGLE2-TR-L9b

would have been sufficient to claim the presence of a transiting extrasolar planet, although with an unknown mass. Similar arguments may have to be used in the case of future detection of transits of Earth-size planets from Kepler or CoRoT, since their radial velocity signature may be too small to measure.

OGLE2-TR-L9b has a significantly larger radius than expected for a planet of about 4.5 times the mass of Jupiter, even if it is assumed that 0.5% of the incoming stellar luminosity is dissipated at the planet's center (Fressin et al. 2007). However, it is not the only planet found to be too large (e.g. CoRoT-exo-2b, TrES-4b, and XO-3b). Several mechanisms have been proposed to explain these 'bloated' radii, such as more significant core heating and/or orbital tidal heating (see Liu, Burrows & Ibgui 2008 for a recent detailed discussion).

The measured vsini and estimated stellar radius combine to a rotation period of the host star of ~1.97±0.04 days. It means that the rotation of the star is not locked to the orbital period of OGLE2-TR-L9b. A vsini of 39 km/sec is within the normal range for stars of this spectral type. The mean vsini of F5 to F0 stars in the solar neighbourhood range from 10^2 to 10^3 km/sec respectively. Note that the vsini of OGLE2-TR-L9a is only ~9% of the expected break-up velocity for a star of this mass and radius. Assuming the general Roche model for a rotating star (e.g. Seidov, 2004), the ratio of polar to equatorial radius of OGLE2-TR-L9a will be on the order of, $1 - \frac{1}{2}(v/v_{max})^2 \sim 0.996$. Thus, the rotational flattening of the host star is not expected to significantly influence the transit shape. OGLE2-TR-L9 is expected to exhibit a strong Rossiter-McLaughlin effect. Simulation using a segmented stellar surface predict an amplitude of 230 m/sec.

References

Aigrain, S., et al. 2008, A&A Let. in press, arXiv:0807.3767
Anderson, D. R., et al. 2008, MNRAS, 387, L4
Burke, C. J., et al. 2008, ApJ submitted, arXiv:0805.2399
Charbonneau D., Brown T.M., Noyes R.W., Gilligand R.L., 2002, ApJ 568, 377
Charbonneau D., Allen L., Megeath S., Torres G., Alonso R., Brown T., Gilliland R., Latham D., Mandushev G., O'Donovan F., Sozzetti A., 2005, ApJ, 626, 523
Claret, A. 2004, A&A, 428, 1001
Dekker, H. et al. 2000, SPIE, 4008, 534.
Deming, D., Seager, S., Richardson, L. J., & Harrington, J. 2005, Nature, 434, 740
Fressin, F., Guillot, T., Morello, V., & Pont, F. 2007, A&A, 475, 729
Greiner, J., et al. 2008, PASP, 120, 405
Hubeny, I., Lanz, T., & Jeffery, C. S. 1994, SYNSPECa User's Guide, in Newsl. on Analysis of Astronomical Spectra 20 (St. Andrews Univ.)
Knutson, H. A., et al. 2007, Nature, 447, 183
Liu X., Burrows A., Ibgui L., 2008, ApJ, in press, arXiv:0805.1733
Mandel K. & Agol E. 2002, ApJ, 580, L171
Mandushev et al. 2005, ApJ621, 1061
Mandushev, G., et al. 2007, ApJ, 667, L195
Pasquini, L. et al. 2002, The Messenger 110, 1.
Queloz, D., et al. 2001, A&A, 379, 279
Seidov Z., 'The generalized Roche model', 2004, astro-ph/0407174
Shporer, A., et al. 2008, ApJ submitted, arXiv:0806.4008
Siess, L., Dufour, E., & Forestini, M. 2000, A&A, 358, 593
Snellen, I. A. G., van der Burg, R. F. J., de Hoon, M. D. J., & Vuijsje, F. N. 2007, A&A, 476, 1357 (S07)
Snellen, I. A. G., Albrecht, S., de Mooij, E. J. W., & Le Poole, R. S. 2008, A&A, 487, 357
Szymanski, 2005, Acta Astron., 55
Tinetti, G., et al. 2007, Nature, 448, 169
Torres G., Konacki M., Sasselov D., Saurabh J., 2004, ApJ 614, 979
Udalski, A., Kubiak, M., & Szymanski, M. 1997, Acta Astronomica, 47, 319

Udalski, A., et al. 2008, A&A, 482, 299